Preprints.org

Article

Not peer-reviewed version

# Photodynamic Therapy in Combination with Cisplatin Chemotherapy Showed Improved Anticancer Efficacy over the Corresponding Photosensitizer-Cis- or Trans-Platin Conjugates in Treating Lung, Head /Neck Cancer Cell Lines and Tumor Models

Mykhaylo Dukh , Farukh A. Durrani , Joseph Cacaccio , Walter A. Tabaczynski , Mehrgan Ghazaeian , Paras N. Prasad , Heinz Baumann * , Ravindra K. Pandey *

Posted Date: 19 June 2026

doi: 10.20944/preprints202606.1473.v1

Keywords: photosensitizer (PS); photodynamic therapy (PDT); structure activity relationship (SAR); FDG; fluorodeoxyglucose

Preprints.org is a free multidisciplinary platform providing preprint service that is dedicated to making early versions of research outputs permanently available and citable. Preprints posted at Preprints.org appear in Web of Science, Crossref, Google Scholar, Scilit, Europe PMC, OpenAlex.

Copyright: This open access article is published under a Creative Commons CC BY 4.0 license, which permit the free download, distribution, and reuse, provided that the author and preprint are cited in any reuse.

Preprints.org (www.preprints.org) | NOT PEER-REVIEWED | Posted: 19 June 2026 doi:10.20944/preprints202606.1473.v1

Disclaimer/Publisher's Note: The statements, opinions, and data contained in all publications are solely those of the individual author(s) and contributor(s) and not of MDPI and/or the editor(s). MDPI and/or the editor(s) disclaim responsibility for any injury to people or property resulting from any ideas, methods, instructions, or products referred to in the content.

*Article*

# Photodynamic Therapy in Combination with Cisplatin Chemotherapy Showed Improved Anticancer Efficacy over the Corresponding Photosensitizer-Cis- or Trans-Platin Conjugates in Treating Lung, Head /Neck Cancer Cell Lines and Tumor Models

**Mykhaylo Dukh [1,2], Farukh A. Durrani [1,2], Joseph Cacaccio [1], Walter A. Tabaczynski [1], Mehrgan Ghazaeian [2], Paras N. Prasad [2], Heinz Baumann [3,*] and Ravindra K. Pandey [1,2,*]**

[1] PDT Center, Cell Stress Biology, Roswell Park Comprehensive Cancer Center, Elm and Carlton Streets, Buffalo, NY 14263, USA

[2] Institute of Lasers, Photonics and Bio-Photonics, University at Buffalo, Flint Entrance, Amherst, NY 14260, USA

[3] Department of Molecular Biology, Roswell Park Comprehensive Cancer Center, Elm and Carlton Streets, Buffalo, NY 14263, USA

* Correspondence: uhbaumann@hotmail.com (H.B.); rkpandey@buffalo.edu or ravndra.pandey@roswellpark.org (R.K.P.)

**Abstract**

To investigate the therapeutic potential of cisplatin chemotherapy in combination with photodynamic therapy (PDT), HPPH [3-(1'-hexyloxy) ethyl)-3-devinyl-pyropheophorbide-a] was conjugated with both *cis*- and *trans*-platins. Both the conjugates showed lower cellular uptake and cell kill than HPPH under similar drug doses and light treatment parameters. In contrast, HPPH at a dose of 0.47 mmol/kg showed 20% anticancer activity on day 60 in mice bearing either head & neck or lung cancer (NSCLC). Interestingly, HPPH-PDT in combination with cisplatin chemotherapy resulted in 80% tumor cure on day 60. This combinatorial approach was further extended to SCID mice implanted with patients' lung tumors derived and treated with not radioactive iodinated HPPH (PS-531, a corresponding PS with 124I isotope, is under IND submission to the United States FDA 's approval for Phase I clinical trial of lung cancer imaging in patients by PET). Like HPPH, PS-531 also exhibited excellent tumor cure (80%) on day 60. Interestingly, PS 531-mediated PDT followed by treatment with cisplatin at a reduced chemotherapy dose gave 100% tumor cure in mice bearing lung cancer on day 60.

**Keywords:** photosensitizer (PS); photodynamic therapy (PDT); structure activity relationship (SAR); FDG; fluorodeoxyglucose

## 1. Introduction

Among the chemotherapy agents approved by the Food and Drug Administration (FDA) to treat cancer, cisplatin is one of the most widely used anticancer agents [1]. It is used all over the world in clinics to treat multiple solid tumors, e.g., testicular, bladder and lung [2]. Like many chemotherapy agents, resistance to cisplatin, whether intrinsic (present before treatment) or acquired (developing during therapy), remains a major obstacle to its long-term clinical effectiveness [3]. Tumor cells employ a multifaceted array of mechanisms to evade cisplatin-induced cytotoxicity, which involve alterations in drug transport, detoxification, DNA repair, and cell death pathways [4]. Some of the

© 2026 by the author(s). Distributed under a Creative Commons CC BY license.

Preprints.org (www.preprints.org) | NOT PEER-REVIEWED | Posted: 19 June 2026 doi:10.20944/preprints202606.1473.v1



major cisplatin toxicity include nephrotoxicity (acute kidney injury), ototoxicity (hearing loss, tinnitus), neurotoxicity (peripheral neuropathy) and myelosuppression (anemia, leukopenia, thrombocytopenia) [5]. Compared to other chemotherapy agents, cisplatin shows a favorable pharmacokinetic profile, therefore, it is still used in clinics, and strategies applied to enhance its efficacy with reduced toxicity [6]. Thus, efforts to improve the therapeutic index are underway in various but laboratories by designing rational combination therapies and/or increasing its delivery to tumor cells [7]. To achieve maximal benefit by using combinational therapy, the treatment parameters should be rationally designed to have different mechanistic action for destroying tumors and are synergistic, not antagonistic, and should not have additive toxicity profiles.

Given the high incidence and mortality from lung cancer, there have been improvements in surgery, radiation therapy and chemotherapy, which are the main treatment modalities available to patients [9]. Nevertheless, there has been limited change in lung cancer survival in the last decade. Molecularly targeted therapy is promising, but only a small fraction of patients has targetable mutations. Thus, the need for additional therapeutic modalities remains high [10]. Surgery remains the primary treatment modality for loco-regional disease. However, local recurrence remains a significant problem despite modest improvement in survival from adjuvant chemotherapy. Due to the association of lung cancer with tobacco use many patients also suffer from impaired lung function resulting from chronic obstructive pulmonary disease (COPD) [11]. Consequently, surgical resection of some early-stage tumors may be contraindicated because of inadequate pulmonary reserve. Additionally, up to 10% of successfully resected or radiated lung cancer subsequently develop a second primary lung neoplasm, and another operation or further radiotherapy may not be feasible at that point. Thus, therapeutic approaches that spare functional lung tissue are required for many patients in whom lung cancer is diagnosed [12].

PDT has been used successfully for endobronchial palliation of advanced disease and for the management of early lung cancer [13]. The fact that PDT works well in combination with other oncologic procedures and therapies makes this an important tool in the modern multidisciplinary approach to thoracic malignancies [14]. In PDT, systemic administration of a light-activatable drug (i. e. photosensitizer, PS) followed by illumination of the target tissue with visible light produces reactive oxygen species (mainly singlet oxygen), resulting in tumor cell death, microvasculature damage and local inflammation. This treatment modality has remained a promising approach in thoracic oncology for quite some time [15]. It is an established therapy for obstructive or premalignant lesions in the tracheobronchial tree. The relative simplicity of this intervention and its highly reliable tumor ablative ability, make it attractive as a therapeutic modality for broader application in lung cancer [16]. However, the major side effects of skin phototoxicity and the relatively superficial nature of tumor necrosis produced by this modality have contributed to the limited application of PDT in lung cancer [17]. Therefore, photosensitizers with improved photophysical properties, higher tumor-specificity, limited skin phototoxicity and fluorescence-guided PDT have been currently the objectives of various laboratories [18].

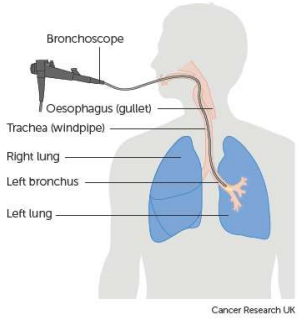


**Figure 1.** Illustration of the treatment of lung cancer patients by Photodynamic Therapy (PDT).

© 2026 by the author(s). Distributed under a Creative Commons CC BY license.

Preprints.org (www.preprints.org) | NOT PEER-REVIEWED | Posted: 19 June 2026 doi:10.20944/preprints202606.1473.v1



Since the approval of Photofrin™ by the United States FDA (US FDA) for its use in clinical PDT, both active and passive approaches of developing agents related to porphyrins and non-porphyrin with improved tumor-specificity, limited skin phototoxicity and desired photophysical properties have been reported [19]. Among the PSs developed based on structure-activity-relationship (SAR), it was observed that the overall lipophilicity of the molecule plays an important role in its tumor-specificity, tumor retention and pharmacokinetic (PK) profile [20]. For porphyrin-based compounds in which one of the pyrrole ring was reduced (*trans*-), the starting compounds were either isolated from the naturally occurring materials or the desired PS was synthesized starting from pyrroles in a multistep synthesis [21].

## 2. Materials and Methods

**Chemistry:**

***Synthesis of Compound 1.*** HPPH (50.0 mg; 1 eq.) and (benzotriazol-1-yloxy) triprolidine-phosphonium hexafluorophosphate (2.5 eq.) were dissolved in dry DMF (7 ml) under Ar atmosphere. To this solution 4-aminomethyl pyridine (2.5 eq.) and triethylamine (2.5 eq.) were added, and the reaction mixture was stirred overnight at room temperature. After this, reaction mixture was diluted with 30 ml of DCM, and it was washed with $H_2O$ (3 x 30 ml) and dried over $Na_2SO_4$. After filtration the solvent was removed under reduced pressure. The resulting residue was purified by preparative TLC (2 plates), using 6% MeOH in DCM as eluent to give compound **1** in 73% (42 mg) yield. UV-Vis $\lambda_{max}$ (MeOH) : 660 (rel. intensity 0.407), 604 (0.074), 536 (0.081), 504 (0.078), 406 (0.799); $^1$H NMR (400 MHz, $CDCl_3$, δ ppm): 9.80/9.78 (1H, s, 5-H), 9.19/9.18 (1H, s, 10-H), 8.51 (1H, s, 20-H), 8.27 (2H, m, pyridine 2-H & 6-H), 6.79 (2H, m, pyridine 3-H & 5-H), 5.91/5.89 (1H, q, *J* = 6.8 Hz, 3$^1$-H), 5.72/5.70 (1H, t, *J* = 5.9 Hz, amide NH), 5.16 (1H, d, *J* = 19.7 Hz, 13$^2$-C*H*H), 5.00/4.99 (1H, d, *J* = 19.7 Hz, 13$^2$-CH*H*), 4.51 (1H, qd, *J* = 7.2, 1.1 Hz, 18-H), 4.32 (1H, m, 17-H), 4.15/4.13 (1H, dd, *J* = 15.8, 6.2 Hz, -C(=O)NHC*H*H-), 3.99/3.95 (1H, dd, *J* = 15.8, 5.7 Hz, -C(=O)NHCH*H*-), ~3.67/3.61 (2H, m, -OC*H*$_2$(CH$_2$)$_4$CH$_3$), ~3.59 (2H, m, 8-C*H*$_2$CH$_3$), 3.37/3.36 (3H, s, 2-CH$_3$), 3.271/3.265 (3H, s, 7-CH$_3$), 3.24/3.22 (3H, s, 12-CH$_3$), 2.65 (1H, m, 17-C*H*HCH$_2$-), 2.51 (1H, m, 17-CH*H*CH$_2$-), 2.27 (1H, ddd, *J* = 14.6, 9.6, 6.4 Hz, 17-CH$_2$C*H*H-), 2.11 (3H, d, *J* = 6.6 Hz, 3$^1$-CH$_3$), 1.93 (1H, ddd, *J* = 14.7, 9.8, 5.3 Hz, 17-CH$_2$CH*H*-), 1.791/1.788 (3H, d, *J* = 7.2 Hz, 18-CH$_3$), ~1.74 (2H, m, -OCH$_2$C*H*$_2$(CH$_2$)$_3$CH$_3$), 1.62/1.61 (3H, t, *J* = 7.6 Hz, 8-CH$_2$C*H*$_3$), 1.39 (2H, m, -O(CH$_2$)$_2$C*H*$_2$(CH$_2$)$_2$CH$_3$), 1.24 (4H, m, -O(CH$_2$)$_3$(C*H*$_2$)$_2$CH$_3$), 0.80/0.78 (3H, distorted t, *J* ~ 7 Hz, -O(CH$_2$)$_5$C*H*$_3$), 0.47 (1H, br s, core NH), -1.66 (1H, s, core NH); $^{13}$C {$^1$H} NMR (100 MHz, $CDCl_3$, δ ppm): 196.1, 172.4, 171.84/171.82, 159.99/159.98, 155.37/155.35, 150.8, 149.7/149.6 (2C), 148.9, 147.2/147.1, 145.11/145.09, 141.5/141.4, 139.89/139.87, 137.6/137.5, 136.27/136.25, 135.68/135.66, 132.4/132.3, 130.13/130.12, 128.01/127.99, 122.12/122.10 (2C), 105.94/105.92, 104.02/104.01, 98.1/98.0, 92.5, 72.84/72.81, 69.74/69.73, 51.58/51.56, 50.1, 48.0, 42.14/42.12, 32.52/32.50, 31.74/31.72, 30.23/30.20, 30.21, 26.09/26.07, 24.71/24.66, 23.03/23.02, 22.58/22.56, 19.4, 17.4/17.3, 14.0/13.9, 11.70/11.69, 11.3, 11.03/11.02. HRMS (ESI) calculated for $C_{45}H_{55}N_6O_3$ [MH$^+$] 727.4336, found 727.4352

***Synthesis of Compounds 2 and 3.*** These compounds were obtained by following a previously published procedure*. Silver nitrate, ($AgNO_3$, 5.0 mg), was added to the solution of trans- or cisplatin (9.0 mg) in DMF (4.0 ml), and the reaction mixture was stirred overnight in darkness under Ar atmosphere at 55$^o$C. Then AgCl precipitate was filtered, compound **1** (20.0 mg) was added to supernatant, and reaction was stirred under the same conditions as described above. After this DMF was removed under high vacuum and residue was dissolved in MeOH. Unreacted trans- or cisplatin was filtered off, solvent was evaporated under reduced pressure and desired product (compound **2** or **3** accordingly) was purified by silica column chromatography, using gradient 5-8% of MeOH in DCM as eluent. Title compounds were obtained in 69% (20.0 mg) yield each.

***Characterization of compound 2:*** UV-Vis $\lambda_{max}$ (MeOH) : 660 (rel. intensity 0.130), 605 (0.026), 536 (0.029), 504 (0.029), 406 (0.261); $^1$H NMR (400 MHz, 93:7 $CDCl_3$/$CD_3OD$, δ ppm): 9.64/9.63 (1H, s, 5-H), 9.28 (1H, s, 10-H), 8.52 (2H, m, pyridine 2-H & 6-H), 8.44 (1H, s, 20-H), 7.18 (2H, m, pyridine 3-H & 5-H), 5.82/5.80 (1H, q, *J* = 6.7 Hz, 3$^1$-H), 5.14/5.13 (1H, d, *J* = 19.9 Hz, 13$^2$-C*H*H), 4.94 (1H, d, *J* = 19.9

© 2026 by the author(s). Distributed under a Creative Commons CC BY license.

Preprints.org (www.preprints.org) | NOT PEER-REVIEWED | Posted: 19 June 2026 doi:10.20944/preprints202606.1473.v1



Hz, 13²-CH*H*), 4.45 (1H, qd, *J* = 7.3, 1.7 Hz, 18-H), 4.32/4.30 (1H, d, *J* = 16.6 Hz, -C(=O)NHC*H*H-), 4.21 (1H, m, 17-H), 4.21/4.19 (1H, d, *J* = 16.5 Hz, -C(=O)NHCH*H*-), ~3.59/3.52 (2H, m, -OC*H*₂(CH₂)₄CH₃), ~3.56 (2H, m, 8-C*H*₂CH₃), 3.45 (3H, s, 12-CH₃), ~3.29 (3H, s, 2-CH₃), 3.16 (3H, s, 7-CH₃), ~2.60 (1H, m, 17-C*H*HCH₂-), ~2.54 (1H, m, 17-CH₂C*H*H-), ~2.27 (1H, m, 17-CH₂CH*H*-), ~2.20 (1H, m, 17-CH*H*CH₂-), 2.024/2.017 (3H, d, *J* = 6.7 Hz, 3¹-CH₃), 1.73 (3H, d, *J* = 7.2 Hz, 18-CH₃), ~1.66 (2H, m, -OCH₂C*H*₂(CH₂)₃CH₃), 1.584/1.581 (3H, t, *J* = 7.6 Hz, 8-CH₂C*H*₃), 1.29 (2H, m, -O(CH₂)₂C*H*₂(CH₂)₂CH₃), 1.13 (4H, m, -O(CH₂)₃(C*H*₂)₂CH₃), 0.69 (3H, distorted t, *J* ~ 7 Hz, -O(CH₂)₅C*H*₃); ¹³C {¹H} NMR (100 MHz, 93:7 $CDCl_3/CD_3OD$, δ ppm): 197.2, 174.18/174.16, 172.2, 160.6, 155.7, 152.64/152.61 (2C), 150.8, 148.94/148.92, 145.1, 141.5, 139.58/139.56, 137.2, 136.2, 135.7, 132.6/132.5, 129.5, 127.8, 125.10/125.09 (2C), 105.5/105.4, 104.0, 97.7/97.6, 92.7, 72.7/72.6, 69.6, 51.5, 50.0, 47.8, 41.58/41.56, 32.62/32.59, 31.5, 30.72/30.67, 30.0, 25.9, 24.4/24.3, 22.8, 22.4, 19.2, 17.1, 13.7, 11.7, 11.0, 10.8. Note: The following protons were not observed due to chemical exchange: two core, one amide, and six ammine protons. One carbon (the pyridine moiety C4) produced no observable signal, presumably due to aggregation-induced line broadening. HRMS (ESI) calculated for $C_{45}H_{60}N_8O_3ClPt$ [M⁺] 990.4125, found 990.4146

***Characterization of compound 3****:* UV-Vis $\lambda_{max}$ (MeOH) : 660 (rel. intensity 0.323), 603 (0.060), 536 (0.066), 504 (0.063), 407 (0.634); ¹H NMR (400 MHz, 94:6 $CDCl_3/CD_3OD$, δ ppm): 9.64/9.62 (1H, s, 5-H), 8.98 (1H, s, 10-H), 8.50 (2H, m, pyridine 2-H & 6-H), 8.424/8.420 (1H, s, 20-H), 7.08 (2H, m, pyridine 3-H & 5-H), 5.81/5.79 (1H, q, *J* = 6.8 Hz, 3¹-H), 5.12/5.11 (1H, d, *J* = 19.9 Hz, 13²-C*H*H), 4.91 (1H, d, *J* = 19.8 Hz, 13²-CH*H*), 4.42 (1H, qd, *J* = 7.3, 1.7 Hz, 18-H), 4.17/4.14 (1H, d, *J* ~ 16.7 Hz, -C(=O)NHC*H*H-), ~4.15 (1H, m, 17-H), 4.08/4.07 (1H, d, *J* = 16.7 Hz, -C(=O)NHCH*H*-), ~3.48-3.62 (2H, m, -OC*H*₂(CH₂)₄CH₃), 3.41 (2H, q, *J* = 7.5 Hz, 8-C*H*₂CH₃), 3.27/3.26 (3H, s, 2-CH₃), 3.18 (3H, s, 12-CH₃), 3.15/3.14 (3H, s, 7-CH₃), 2.56 (1H, m, 17-C*H*HCH₂-), 2.42 (1H, m, 17-CH₂C*H*H-), ~2.22 (1H, m, 17-CH*H*CH₂-), ~2.15 (1H, m, 17-CH₂CH*H*-), 2.02/2.00 (3H, d, *J* = 6.7 Hz, 3¹-CH₃), 1.702/1.695 (3H, d, *J* = 7.3 Hz, 18-CH₃), 1.66 (2H, m, -OCH₂C*H*₂(CH₂)₃CH₃), 1.491/1.486 (3H, t, *J* = 7.6 Hz, 8-CH₂C*H*₃), 1.32/1.26 (2H, m, -O(CH₂)₂C*H*₂(CH₂)₂CH₃), 1.14 (4H, m, -O(CH₂)₃(C*H*₂)₂CH₃), 0.70/0.69 (3H, distorted t, *J* ~ 7 Hz, -O(CH₂)₅C*H*₃); ¹³C {¹H} NMR (100 MHz, 94:6 $CDCl_3/CD_3OD$, δ ppm): 197.1, 173.8, 172.2, 160.4, 155.6, 152.5 (2C), 151.72/151.70, 150.7, 148.84/148.82, 145.1, 141.5/141.4, 139.64/139.62, 137.1, 136.12/136.10, 135.7, 132.6/132.5, 129.4, 127.6, 124.4 (2C), 105.48/105.45, 103.8, 97.8/97.7, 92.6, 72.69/72.66, 69.6, 51.5, 50.0, 47.8, 41.5, 32.7/32.6, 31.6, 30.64/30.61, 30.0, 25.9, 24.42/24.36, 22.8, 22.4, 19.1, 17.1, 13.8, 11.5, 11.1, 10.81/10.78. Note: The following protons were not observed due to chemical exchange: two core, one amide, and six ammine protons. HRMS (ESI) calculated for $C_{45}H_{60}N_8O_3ClPt$ [M⁺] 990.4125, found 990.4168

***Formulation of Photosensitizers:*** HPPH: 1 mg and Tween80 (50 ul) were mixed vigorously for 15-20 min using mortar and pestle and left in darkness at room temperature for 4-5 hours covered in foil. The resulting mixture was diluted with 5% dextrose solution (5 ml) and filtered through 0.2-micron filter to remove any bacteria. Concentration of the PS In Tween formulation was calculated spectrophotometry using Beer-Lambert law. A=ecb, where A is absorbance, e is extinction coefficient, c is concentration of compound and b is pathlength of the light through solution (1.0 cm). The concentration of the PS was 0.198 mmol/L (198 umol/L). The iodinated PS (531) was formulated in 2% Pluronic F-127 aqueous solution and the concentration of the PS was measured by following the method discussed for HPPH.

**Biological Studies:**

**In vitro *photosensitizing efficacy by MTT Assay:*** MTT [3-(4,5-Dimethylthiazol-2-yl)-2,5-Diphenyltetrazolium Bromide)] was acquired from ThermoFisher. Standard protocol was followed to determine cell viability after PDT. Briefly, cells were plated in 96 well lates at a concentration of 10k cells per well. The cells were allowed to adhere to the plastic before being exposed to HPPH, compound 2 or compound 3. Cells incubated with the drug formulation for 24 hours before plates were exposed to 1J/cm² of 665 nm light at a dose rate of 3.2 mW/cm². 48 hours post PDT, MTT assay was started by adding 15 µl of MTT solution to each well. After an incubation time of 2 hours, the plates were washed and DMSO was added to solubilize the Formazan salt. Plates were read at 570 nm. Viability was *determined by comparing to control wells on the same plate that received no stressors.*

© 2026 by the author(s). Distributed under a Creative Commons CC BY license.

Preprints.org (www.preprints.org) | NOT PEER-REVIEWED | Posted: 19 June 2026 doi:10.20944/preprints202606.1473.v1



**In vitro *Fluorescence microscopy:*** Approximately 100k NSCLC cells were plated in 6 well plates and allowed to adhere for 24 hours. The wells were washed twice with cold PBS before receiving fresh media with 1 μM of either HPPH, compound 2 or compound 3. 24 hours after the photosensitizer was added, each well was washed twice with ice cold PBS before replacing with phenol red free media. Plates were immediately imaged utilizing a Zies microscope, taking at least 3 different fields. Fields were analyzed by normalizing the red fluorescence from the photosensitizer to the number of cells in the field.

***Method for Tumor Implantation:*** The FaDu tumors were transplanted into 6–8-week-old female SCID mice (Strain C.B Igh-1b Icr Tac Prkdc Scid) and were maintained in the animal facility. Mice bearing an established tumor (~7 days after implantation) were treated with PDT and Cisplatin. Two axes (mm) of tumor (L, longest axis; W, shortest axis) were measured with the aid of a Vernier caliper. It was estimated using a formula: tumor volume = 1/2(L ×W2). The tumors were irradiated with light (fluence: 135 J/cm2; fluence rate: 75 mW/cm2 for 30 min at 665 nm using a Lightwave laser diode. The mice restrained without anesthesia in plexiglass holders designed to expose only the tumor and a 2–4 mm annular margin of skin to light. Tumor measurements were taken daily for first 10 days and then three times a week for 4 weeks, followed by twice a week thereafter for a total of 60 days post treatment. The untreated control was compared for tumor response for each treatment group subjected to PDT ± Cisplatin therapy (CT).

Complete tumor regression (CR) was defined as the inability to detect the tumor by palpation at the initial site of tumor appearance for more than 2 months post therapy. Partial tumor regression (PR) was defined as a ≥ 50% reduction in initial tumor size. Observations of scar formation, edema, erythema, in the treatment field were observed and recorded. All studies were performed in accordance with protocols approved by the institutional animal care and use committee of our institution

***Statistical Analysis:*** The standard log-rank test (Mantel–Cox) was used for statistical analysis. It is a test to compare the survival of the animal/tumor cure based on the Kaplan–Meier survival curve. It detects differences between groups to confirm. For in vivo PDT/CT efficacy analysis the cure rate and the survival curves were plotted using the drug dose over tumor regrowth. This study was conducted in an AAALAC-accredited facility, following the IACUC-approved animal protocol.

## 3. Results and Discussion

**Chemistry**

In our laboratory PDT drug development has been focused on using natural products as starting materials, and most of the compounds for cancer-imaging (fluorescence, PET, MRI) and therapy (PDT, SDT) were derived either from chlorophyll-a or bacteriochlorophyll-a [22]. Among the compounds developed so far, three agents, e.g., (i) 3-(1′-hexyloxyethyl)-3-devinylpyropheophorbide (HPPH, 665 nm, currently in Phase II clinical trials of head & neck [23] and esophageal cancers) [24], (ii) Photobac 787 nm (derived from bacteriochlorophyll-a) is in Phase I clinical trial of Glioblastoma) [25] and (iii) PET-ONCO, an $^{124}$I- analogs derived from chlorophyll-a) for PET-imaging of those cancers (e.g., bladder, brain, kidney) for which F-18 FDG shows limitations [26,27]. Additional advantages of these compounds over Photofrin™ are reduced skin phototoxicity, longer wavelength light adsorption, improved photophysical characteristics, improved anticancer activity and desired PK profile [28,29].

We have previously reported that HPPH is an effective PS for the treatment of a variety of cancers with no significant toxicity in absence of light [22]. Like other PDT PSs, HPPH also shows limitations in treating metastases, whereas for the localized cancer and metastasis, cisplatin, a chemotherapeutic agent has been frequently used. However, in contrast to PDT, recurring cancer cells show resistance to cisplatin chemotherapy [30]. Therefore, our objective was to investigate the potential of PDT in combination with chemotherapy by first conjugating HPPH with cis-platin as multitherapeutic agent (PDT and chemotherapy), and to compare its efficacy in combination of

© 2026 by the author(s). Distributed under a Creative Commons CC BY license.

Preprints.org (www.preprints.org) | NOT PEER-REVIEWED | Posted: 19 June 2026 doi:10.20944/preprints202606.1473.v1



HPPH-PDT followed with cisplatin chemotherapy in vitro using head & neck and NSCLC cell line and in mice, bearing patient's derived tumors.

In the process of optimizing the structural requirements of a drug candidate, it has been reported that structural isomers show a significant impact on therapy due to their binding efficacy of targeted site (s) and the pharmacological parameters, which leads to the development of more effective and safer candidates [31]. In some cases, it is also possible that one isomer could be more effective and less toxic than the other. For example, the anticancer drug cisplatin is a *cis* isomer, while its other form *trans*-isomer shows limited efficacy [32]. However, in case of HPPH, in which pyrrole ring-D is trans reduced, and the presence of a chiral center at position 3(1'-) produces a mixture of two epimers *R*- and *S)*. Both the epimers were separated and investigated separately for in-vitro and in-vivo biological activity resulting to similar efficacy [33], resulting to its approval by the United States FDA for conducting the human clinical trials [34]. Therefore, in present study, HPPH (as an epimeric mixture) was prepared by following our own methodology and used as such. However, to investigate the impact of respective PS-cisplatin conjugate, HPPH was reacted separately with both *cis*- and *trans*-platin by following the reaction sequences shown in Scheme 1. The desired conjugates **2** and **3** were obtained > 70% overall yield, and were characterized by UV-vis, NMR and mass spectrometry analyses (for $^{1}$H NMR spectra of compounds **2** and **3** please see Figure 2. The $^{13}$C-NMR spectra of compounds 1-3 are included in Supporting Information (Figures S1–S3).

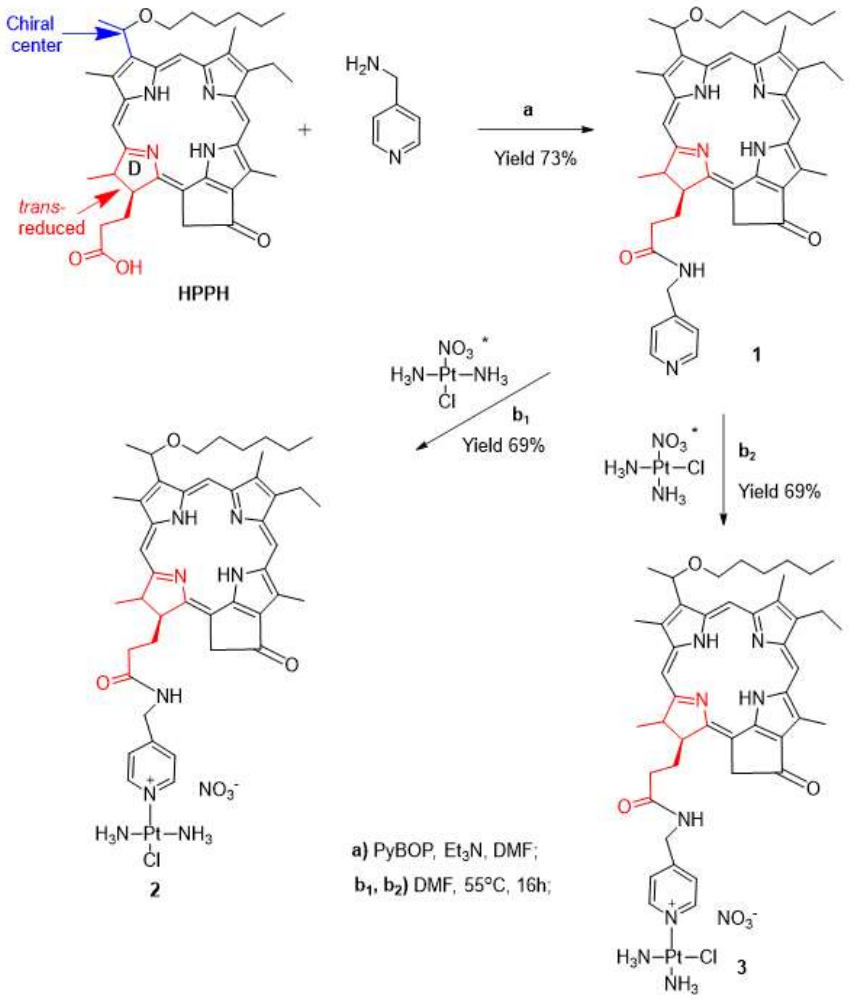


**Scheme 1.** Synthesis of HPPH- transplatin **2** and cisplatin **3** conjugates.

© 2026 by the author(s). Distributed under a Creative Commons CC BY license.

Preprints.org (www.preprints.org) | NOT PEER-REVIEWED | Posted: 19 June 2026 doi:10.20944/preprints202606.1473.v1



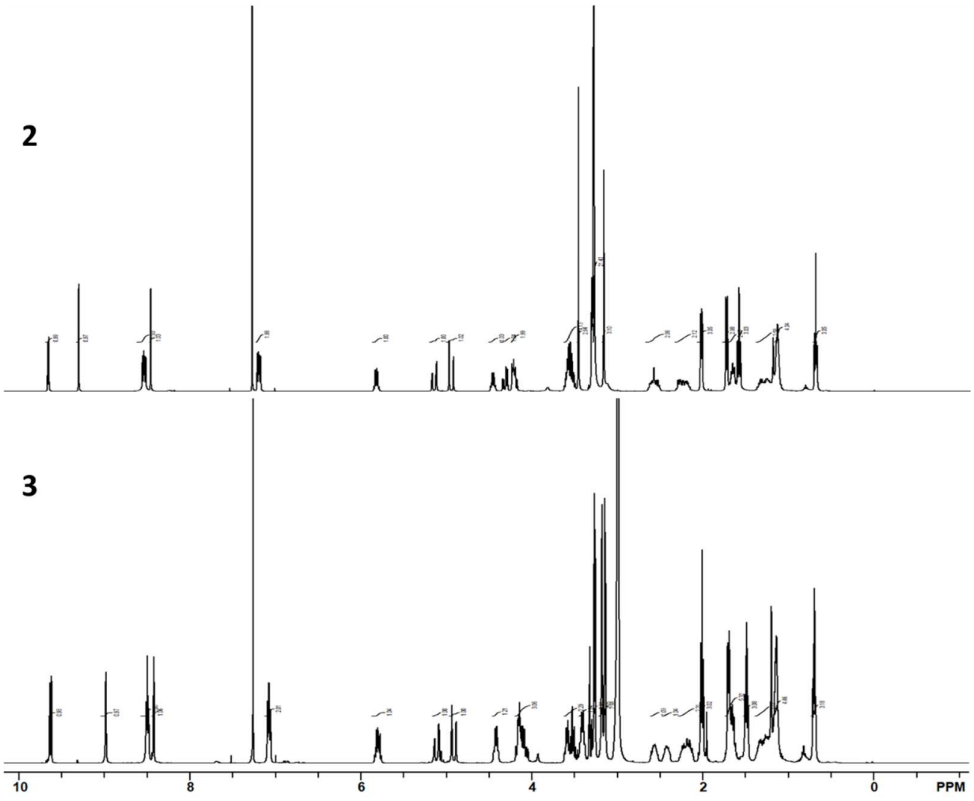


**Figure 2.** The NMR spectra of conjugates **2** and **3** dissolved in $CDCl_3$ were recorded using 400 MHz spectrometer**.**

Conjugation of HPPH with *cis*- and *trans*-platin did not produce any significant impact in its photophysical properties (long wavelength absorption, fluorescence and ROS production). The $^{13}C$ NMR spectra (see Figure 2 and Supporting Materials) of compounds **1**, **2**, and **3** are generally consistent with their proposed structures. Spectral features exhibited by these compounds are similar to those observed for known compounds of like structure. However, selected protons of these three conjugates show significant differences in their $^{1}H$ chemical shifts relative to each other and to the unsubstituted parent compound (HPPH).

In conjugate **1** the 10-H, $13^2$-CH*H*, and 12-$CH_3$ protons were observed at 9.19/9.18, 5.00/4.99, and 3.24/3.22 ppm, respectively. In HPPH, however, these protons appear at 9.46, 5.12, and 3.63 ppm, respectively. So, conjugation to the picolyl group via amide linkage at position 17 results in a significant shielding of each of these protons, which ranged from ~0.1 to ~0.4 ppm. The $17^1$ CH*H* proton (δ = 2.51 ppm) of **1** exhibits a substantial de-shielding (of 0.26 ppm) relative to HPPH (δ = 2.25 ppm). Also, the two $17^2$ methylene protons are shielded (by ~0.4 ppm) in **1** (δ = 2.27 and 1.93 ppm) relative to HPPH (δ = 2.61 and 2.31 ppm).

In **2** (the trans-platin conjugate) the 10-H, $13^2$-CH*H*, and 12-$CH_3$ protons were observed at 9.28, 4.94, and 3.45 ppm, respectively. The proton signal for each of these groups is shielded by ~0.2 ppm relative to the corresponding protons of HPPH. In contrast to **1**, the four 17-$CH_2CH_2$- protons of **2** are slightly shielded (by < 0.1 ppm) compared with HPPH.

For **3** (the cis-platin conjugate) the 10-H, $13^2$-CH*H*, and 12-$CH_3$ protons were observed at 8.98, 4.91, and 3.18 ppm, respectively. Here, the observed shielding ranges from ~0.2 to ~0.5 ppm. The $17^2$ methylene protons show small to moderate shielding (of < 0.2 ppm) relative to HPPH. Lastly, protons of the 8-position ethyl group are moderately shielded compared with HPPH. The 8-C*H*$_2$CH$_3$ protons (δ = 3.41 ppm) are shielded by 0.26 ppm, while the 8-$CH_2$C*H*$_3$ (δ = 1.49 ppm) are shielded by 0.19 ppm.

© 2026 by the author(s). Distributed under a Creative Commons CC BY license.

Preprints.org (www.preprints.org) | NOT PEER-REVIEWED | Posted: 19 June 2026 doi:10.20944/preprints202606.1473.v1



In general, conjugates **1**, **2**, and **3** each exhibit shielding (relative to unconjugated HPPH) of protons in the vicinity of the macrocycle's C-ring. In contrast, protons at sites more distant from the C-ring show little difference in chemical shift. The largest shieldings were observed for the 10-H and 12-$CH_3$ protons, indicating that this region of the macrocycle is the locus of this effect. Smaller shielding was observed for the 8-$CH_2CH_3$ and $13^2$ methylene protons, which are at the fringes of the C-ring region.

Our laboratory previously observed similar phenomena in two other 17-substituted conjugates of HPPH [35] which exhibited shieldings of up to 1.3 ppm (compared to parent HPPH). Like **1**, **2**, and **3**, the previously observed compounds consisted of the HPPH core with a $17^3$ amide linkage to substituents containing aromatic components. In our previous study, we argued that 17-linked substituents can adopt conformations that allow close approach of the substituent's aromatic groups (substituted benzene, quinazoline, and triazole moieties) to the macrocycle's C-ring. Such conformation—which might be stabilized by π-π stacking interactions—could result in ring current induced changes in chemical shifts, like the shieldings we observed in conjugates **1**, **2**, and **3**. Our previous study indicates that 17-linked conjugates may be especially well suited to produce this shielding effect, because similar aromatic substituents linked through other macrocyclic ring positions (e. g., 3- and 20-) failed to produce shielding near the C-ring. We attributed this seemingly unique ability of the 17-linked conjugates to: the proximity between the substituent (at the 17-position) and the site of the C-ring; and to favorable linker length and flexibility.

Differences in chemical shifts of the methylene protons of the 17-$CH_2CH_2$- groups of **1**, **2**, and **3** may simply be due to differences in substituent structure. The largest changes (which range from a deshielding of ~0.25 ppm to a shielding of ~0.30 ppm) in chemical shift of these protons are observed when comparing **1** with parent HPPH. Conversion of the carboxyl group of HPPH to the amide linkage of **1** introduces changes, perhaps through inductive effects, to the electronic environment of the nearby methylene protons. This may account for the observed chemical shift differences. The 17-$CH_2CH_2$- protons of **3** are moderately (by ~0.2 ppm) shielded relative to the corresponding protons in HPPH. The same arguments apply here. That is, conversion of carboxyl to amide can account for the observed shift differences. Other protons of the 17-$CH_2CH_2$- groups of HPPH and the three conjugates exhibit only minor differences in $^1H$ shifts.

When compared to each other, compounds **1**, **2**, and **3** exhibit spectral differences (up to 0.3 ppm) in the protons near the C-ring. The greatest differences are found in the 10-H and 12-$CH_3$ signals. Conjugate **3** (the cis isomer) exhibits the most shielded 10-H and 12-$CH_3$ signals (at 8.98 and 3.18 ppm, respectively), while the most deshielded are those of trans isomer **2** (at 9.28 and 3.45 ppm, respectively). The 8-$CH_2CH_3$ protons of **3** (δ = 3.41 ppm) are moderately shielded compared with those of **1** (δ = 3.59 ppm) and **2** (δ = 3.56 ppm). Other protons near the C-ring show minimal differences in chemical shift among compounds **1**, **2**, and **3**. Chemical shift differences (especially for 10-H and 12-$CH_3$) observed among **1**, **2**, and **3** can perhaps be explained by structural differences that result in differing electronic environments in the three conjugates. The pyridine moiety of **1** is neutral, whereas it is positively charged in both **2** and **3**. Conjugates **2** and **3** differ only in the positions of the groups bound to platinum, with the trans isomer less polar than the cis isomer. These differences in structure and electronic environment may be sufficient to affect the interaction of the 17-substituent with the C-ring region of the macrocycle, resulting in the observed differences in chemical shifts.

***Comparative* in vitro *PDT efficacy in lung cancer cell lines:*** For determining the efficacy of cisplatin conjugated in vitro, a cytotoxicity assay was conducted in a NSCLC cell line comparing HPPH to the compound **2** (HPPH-*tran*-splatin) and **3**. (HPPH-cisplatin) Briefly the cells were incubated in a 96 well plate and exposed to various doses of a single photosensitizer. After 24 hours, the plates were exposed to 1J/$cm^2$ of 665 nm light. The cytotoxicity of each photosensitizer was measured utilizing an MTT assay [36]. The nonconjugated PS (HPPH) with the lowest $IC_{50,}$ was significantly more effective than the corresponding *cis*- and *trans*- platin conjugates (Figure 3).

© 2026 by the author(s). Distributed under a Creative Commons CC BY license.

Preprints.org (www.preprints.org) | NOT PEER-REVIEWED | Posted: 19 June 2026 doi:10.20944/preprints202606.1473.v1



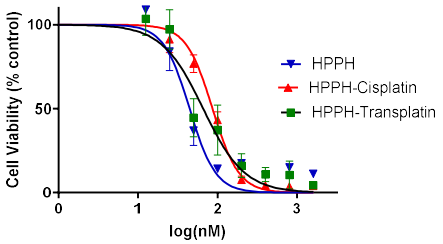


| HPPH | IC50 (nM) |
|---|---|
| HPPH | 44.6 +/- 6.5 |
| HPPH-Cisplatin | 86.5 +/-0.3 |
| HPPH-Transplatin | 66.1 +/- 12.4 |

**Figure 3.** Cytotoxicity of Photosensitizer in NSCLC. Curves were produced utilizing an MTT assay 48 hours post 1J/cm$^2$ exposure. Curves were produced in GraphPad Prism, and the calculated $IC_{50}$ is reported in a tabulated form.

***Comparative cell-uptake and Intracellular localization of HPPH vs HPPH-trans-platin 2 and HPPH-cisplatin 3 in lung cancer and head & neck cancer cell lines:*** The spectral properties of *trans*- and *cis*platin-modified pheophorbide derivatives remained the same as determined for the starting compound HPPH. Hence, we used the fluosescence emitted at 665 nm excitation as measure for the PS level associated with both cancer cells types.

***Studies with lung cancer cell lines:*** Fluorescence microscopy was used to investigate the impact of cellular uptake of each compound to contextualize the results from the cytotoxicity assay. Briefly, cells were allowed to adhere in a 6 well plate for 24 hours before the cell were exposed to one of the PSs. The cells incubated with the selected PS for 24 hours before being washed twice with PBS and imaged with a Zeiss fluorescent microscope. The images are composite of the fluorescence of Hoechst-33342 (blue) and the photosensitizer (red). The graph compares the relative fluorescence of the PS normalized to the number of cells within the field. The bar graph displays the average of three randomly selected fields. As expected, based on our previous studies, HPPH has the highest uptake within the cells after 24 hours [37]. Interestingly, the two platinum conjugates, PS **2** and PS **3**, did not have a significant difference in uptake at 24 hours Figure 3), but compared to both *cis*- or *trans*-platin conjugates, HPPH had significantly higher uptake in lung cancer cells and thus increased cell-killing efficacy. A direct correlation between the tumor cell-uptake and PDT efficacy was observed.

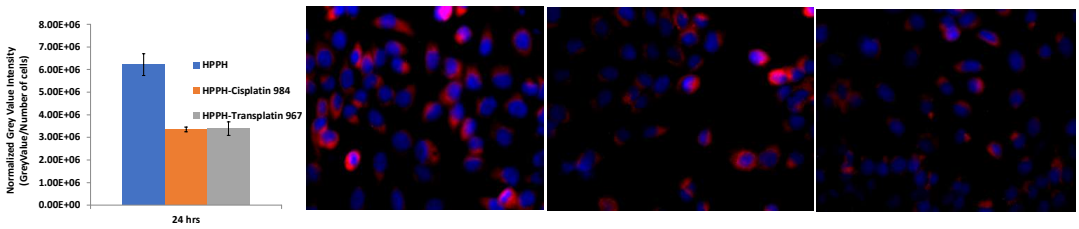


**Figure 4.** Fluorescence images displaying uptake of photosensitizers within NSCLC cells. Cells are co- stained with Hoechst 33342 (blue). The relative fluorescence is graphed on the right, normalizing the photosensitizer fluorescence by the number of cells in each field analyzed. Graph displays triplicate measurements.

***Studies with head & neck cancer cell lines:*** For cell-uptake and biodistribution studies with time, the fluosescence emitted by the PSs at 665 nm excitation served as measure for the PS level associated with test head/neck cancer cells. The fluorescence microscopic images also allowed monitoring the process of cellular uptake, retention and intracellular localization. Initial binding to the plasma membrane was visualized after 30-minute incubation with PS, followed by monitoring transmembrane diffusion and intracellular deposition during a PS-free chase period of up to 48 hours. The quantification of the fluorescence signals indicated that uptake of **PS 2 (PS-985 )** by HNT1 cells was 50% lower than of HPPH (Figure 5, note the different times for recording fluorescence). Moreover, compared to HPPH, **PS2** showed a slower release from the extracellular glycoconjugate structures at the plasma membrane and, hence, delayed trans-plasma membrane difussion and translocation to intracellular structures (Figure 5). The ability of **PS 2** to bind to extracellular

© 2026 by the author(s). Distributed under a Creative Commons CC BY license.

Preprints.org (www.preprints.org) | NOT PEER-REVIEWED | Posted: 19 June 2026 doi:10.20944/preprints202606.1473.v1



membrane components was particularly noted in high-density HN cell cultures, which are characterized by an enhanced deposition of glycoconjugates at the cell surface (Figure 6).

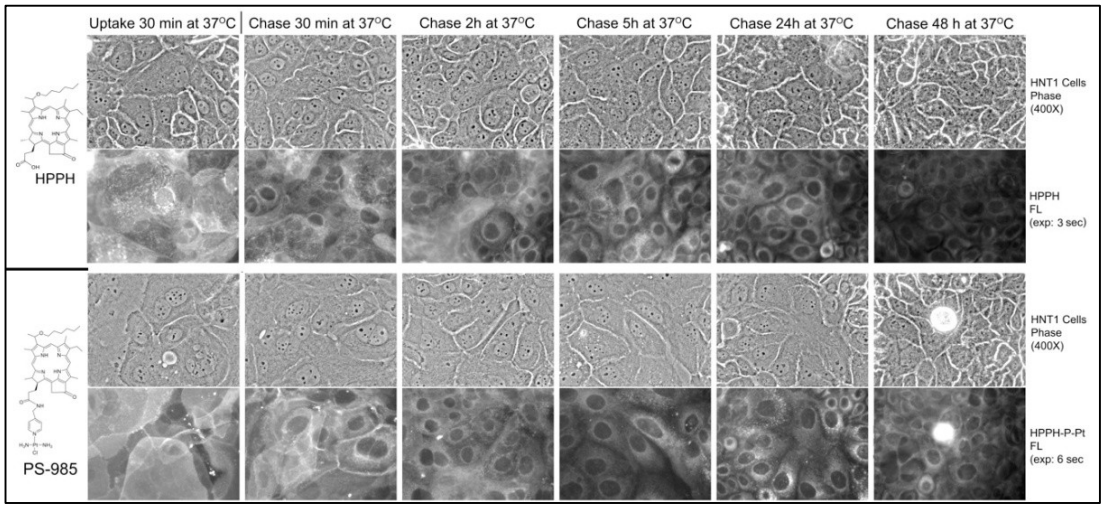


**Figure 5.** Uptake and retention of HPPH and the corresponding *trans*platin conjugate **2** (**PS985**) in HNT 1 cells.

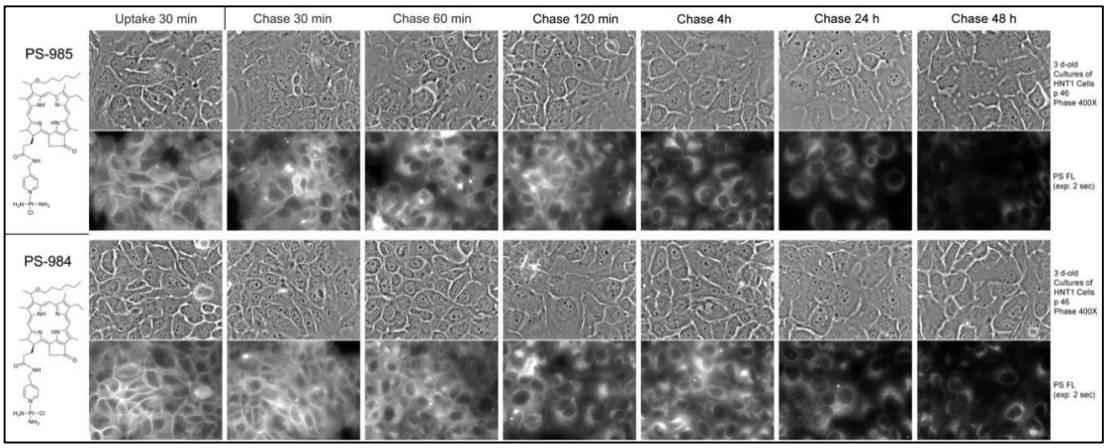


**Figure 6.** Cell surface of PS2 (PS-985) is affected by the formation of the extracellular glycoconjugate coat formed by certain epithelial cells. The amount of extracellular coat is enhanced in densely grown HNT1 cell cultures.

Moreover, **PS 2 (coded as PS 985)**, despite its lower uptake, showed a more prolonged intracellular retention than HPPH, as evident by the presence fluorescence during the chase periods. Considering that cisplatin and not transplatin served as effective anticancer drug, the cellular uptake and intracellular distribution of HPPH-cisplatin **PS 3 (coded as 984)** was compared to HPPH-transplatin **PS 2** in HNT1 cultures (Figure 7). Stable binding of HPPH conjugated with *trans*platin **2 (coded PS-985)** to intracellular structures of HNT1 cells was observed and shown in Figure 8. Comparable uptake kinetics and subcellular distribution of both compounds were observed. Again, no appreciable association of cisplatin-conjugated **PS 3 (coded as 984)** with nuclei was detected and,thus, contrasted to free cisplatin. The predominant cytoplasmic sites of platin-PS retention were mitochondria as previously documented for HPPH37 Figure 9, right panel confirms the mitochondrial co-localization for PS 3, coded as 984).

The action of cisplatin in part has been attributed for its ability binding to DNA, but also to interact with proteins [38]. In order to identify whether **PS 3 (coded as PS-984)** was subject to forming covalent binding to cellular target structures, HPPH- and PS-984-loaded cells after 24 hours chase period were subjected to methanol fixation and extraction. Methanol extraction completely removed

© 2026 by the author(s). Distributed under a Creative Commons CC BY license.

Preprints.org (www.preprints.org) | NOT PEER-REVIEWED | Posted: 19 June 2026 doi:10.20944/preprints202606.1473.v1



all HPPH, resulting in eliminating all fluorescence from cell cultures. In contrast, **PS 3 (coded PS984)** remained bound to mitochondrial and ER structures (Figure 8).

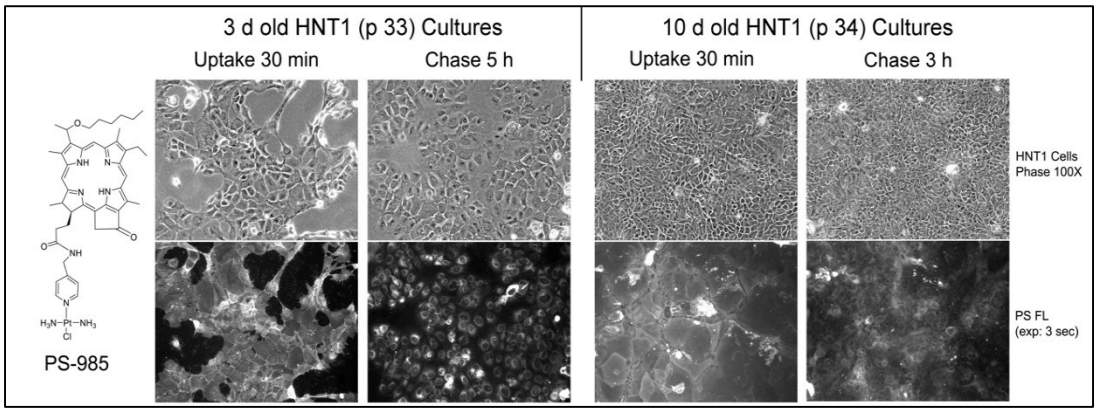


**Figure 7.** Comparative uptake and retention of HPPH-*trans* (**PS2, coded as PS985**) and HPPH-cis-platin (**PS3, coded as PS984**) in HNT1 cells.

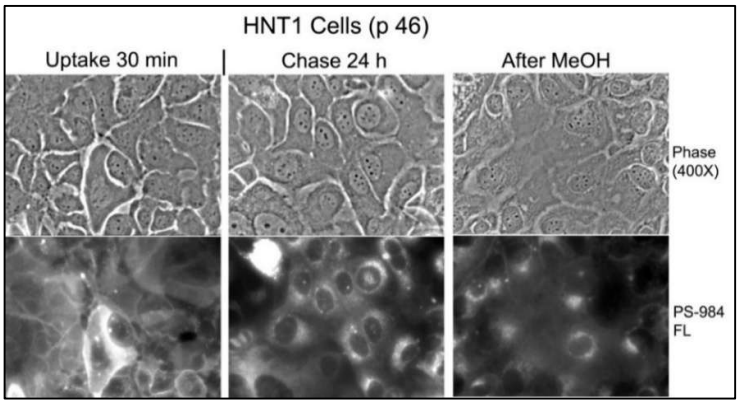


**Figure 8.** Stable binding of HPPH conjugated with *trans*platin **3** (**coded PS-984**) to intracellular structures of HNT1 cells.

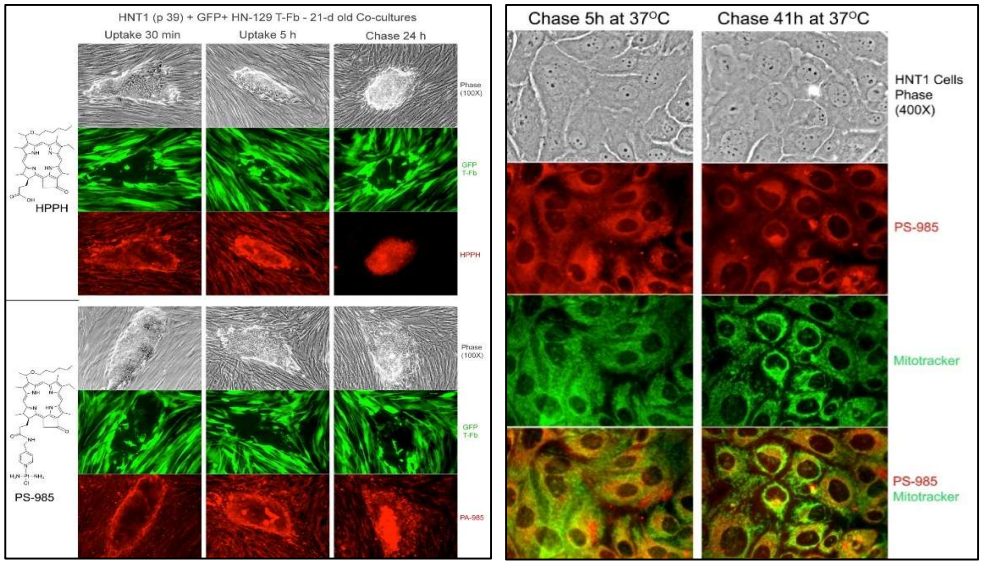


**Figure 9.** Comparative intracellular localization of HPPH and the corresponding transplatin conjugate **2** (**coded as PS 985**) in H & N cancer cell line.

© 2026 by the author(s). Distributed under a Creative Commons CC BY license.

Preprints.org (www.preprints.org) | NOT PEER-REVIEWED | Posted: 19 June 2026 doi:10.20944/preprints202606.1473.v1



A previous detailed analysis of the cell type-specificity of pyropheophorbides has indicated a notable preference for retention by certain epithelial tumor cells compared to co-resident tumor stromal fibroblasts [39] This property could also be confirmed for **PS 2 (coded as PS-985)** using three-dimensional co-culture of head/neck tumors. The cell type-specific association of **PS 2** was visualized by constructing 3D cultures included GFP-tagged HN tumor fibroblasts that outlined the position of the cocultured epithelial tumor cell clusters. Intracellular distrubution pattern of **PS 2** was similar to that of HPPH, with substantial co-localization to mitochondria (Figure 9, left panel). This comparison also indicated that both HPPH and **PS 2** are retained by HNT1 cells at higher level than by fibroblasts. Yet, the tumor-cell specificity of **PS 2** was not as strong than seen with HPPH resulting in an elevated level detectable in fibroblasts after prolonged chase period.

**Comparative in vivo HPPH-PDT in combination with cisplatin chemotherapy:** Since HPPH-*cis*- and *trans*-platin conjugates showed limited activity in vitro, these conjugates were not evaluated for in-vivo efficacy. We have previously investigated the in vivo PDT efficacy of HPPH and other chlorophyll-a analogs in mice bearing lung, head and neck FaDu xenografts as well as other tumor types, the most effective drug dose was 0.47 mmol/kg, and light dose was 135 J/cm$^2$, 75 was 0.47. Therefore, the same treatment parameters were used to investigate the long-term tumor cure by PDT with and without chemotherapy in mice. The regrowth of tumors was followed by 60 days post-PDT treatment, and palpable tumors were monitored via caliper measurement. Tumor volume was measured before the treatment. To investigate the impact of PDT treatment with cisplatin, the PDT treated mice after 1 hour post PDT were injected intra-peritoneally with cisplatin at a dose of 2.5–5 mg/kg (single treatment vs weekly once for 3 weeks). Tumor regrowth was monitored daily for 60 days after the treatment. If there was any tumor regrowth during the tumor response observation period, the mice were euthanized on that day. On day 60, mice with no tumor regrowth (cure) were also euthanized following the animal protocol approved by the IACUC committee. The results obtained from in vivo studies with HPPH-PDT with and without cisplatin chemotherapy are summarized in Table 1. The cure rate (CR) in lung xenograft tumors with HPPH-PDT was 20% (1/5 mice was tumor free on day 60), and in combination with cisplatin a significant increase in tumor response was observed, and 80% (8/10 mice showed complete cure, with a significant P value calculated by Mantel-Cox software in both treatment types.

**Table 1.** HPPH-PDT response in mice bearing lung (NSCLC) or Head & Neck tumors with and without cisplatin.

| Treatment | Tumor (PDX) | HPPH Dose | Cisplatin Dose | Light Dose | Tumor Response (%) | |
|---|---|---|---|---|---|---|
| | | | | | Partial | Complete (Day 60) |
| HPPH-PDT + Cisplatin | NSCLC | 0.47 mmol/kg | 5 mg/week x 3 weeks | 665 nm 135 J/cm$^2$ 75mW/cm$^2$ | 100% (day 7) | 8/10 = 80% (5 mice x 2 groups) |
| HPPH-PDT | NSCLC | 0.47 mmol/kg | None | 665 nm 135 J/cm$^2$ 75mW/cm$^2$ | 100% (day 7) | 1/5 = 20% (5 mice/group) |
| HPPH-PDT + Cisplatin | Head & Neck | 0.47 mmol/kg | 5 mg/week x 3 weeks | 665 nm 135 J/cm$^2$ 75mW/cm$^2$ | 100% (day 7) | 3/5 = 60% (5 mice/group) |
| HPPH-PDT | Head & Neck | 0.47 mmol/kg | None | 665 nm 135 J/cm$^2$ 75mW/cm$^2$ | 100% (day 7) | 1/5 = 20% (5 mice/group) |

The tumor-uptake and in vivo biodistribution of HPPH was also determined in mice treated with the therapeutic dose (0.47 mmol/kg). The best tumor images of SCID mice bearing bilateral

© 2026 by the author(s). Distributed under a Creative Commons CC BY license.

Preprints.org (www.preprints.org) | NOT PEER-REVIEWED | Posted: 19 June 2026 doi:10.20944/preprints202606.1473.v1



tumors were observed at 24 h post injection of the PS, and the biodistribution studies showed a significantly higher uptake in tumor than liver, lung, heart, kidney and spleen at 24 h postinjection.

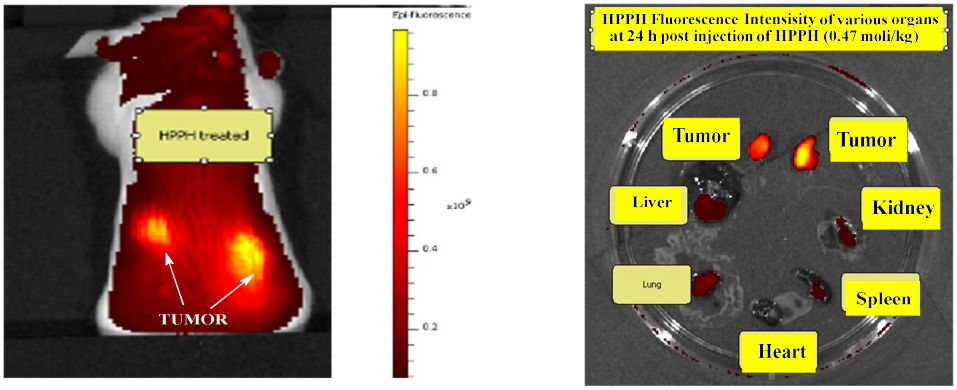


**Figure 10.** (A) Whole body fluorescence image of HPPH (0.47 mmol/kg) in a SCID mouse bearing bilateral lung tumor (NSCLC). (B); Fluorescence intensities of tumors (bilateral), liver, lung, heart, spleen, kidney dissected at 24 h post-injection of the PS. Excitation wavelength range set at 640-675 nm, Emission wavelength range set at 680-740 nm.

The objectives of past and ongoing research in our laboratory has been to develop multifunctional agents for cancer-imaging, including PET, MRI, fluorescence, photoacoustic and PDT [40]. In one of such attempts, discussed that certain iodinated PSs in its radioactive form ($^{124}$I-) can be used for PET imaging of almost all the cancer types, including those, where $^{18}$F-FDG shows limitations (e. g. bladder, brain, kidney and pancreas). The corresponding non-radioactive form the **PS 531** also shows PDT response compared to non-iodinated compounds. Besides, due to its long wavelength optical properties in NIR region, with a significant shift between absorption and fluorescence, it shows a potential for using fluorescence-guided therapy. In a comparative study with Photofrin, the iodinated **PS 531** showed improved antitumor efficacy with limited skin phototoxicity [28]. The IND submission of the iodinated PS to the United States FDA for Phase I human clinical trial is currently underway. The proposed study discussed in the clinical protocol includes two arms study: (i) iodinated PS-PDT and (ii) iodinated PS-PDT with chemotherapy. Before submitting the revised IND application, it was advised by the clinician to conduct an in vivo experiment on iodinated PS with cisplatin using lung cancer patients derived tumors in animal model. To determine the time of optimal of the PS before light therapy. The **PS 531** (1 mmol/kg) was injected intravenously into tumored mice, and the mice were imaged by IVIS spectrum (excitation wavelength range set at 640-675 nm, and emission wavelength range set at 680-740 nm) at variable time points. The uptake of the iodinated PS in tumor, liver and skin is shown in Figure 11. As can be seen, with time there was a significant uptake of the PS in tumor compared to other organs, and the maximum tumor uptake was observed at 24h to 48 h post-injection of the PS (3 mice/group).

Once the optimal time for tumor-uptake of the iodinated PS (1.0 mmol/kg, injected *i.v.)* was determined, the mice bearing lung patients derived tumors were treated with light under the same treatment parameters used for HPPH due to their similar photophysical characteristics. The cure rate in lung xenografts with iodinated **PS 531** was 50% (7/14 mice were tumor free), and in combination with cisplatin the cure rate was 90% (9/10 mice were tumor free) on day 60 with a significant P value of < 0.0001 calculated by Mantel-Cox software in both treatment types (Figure 11 A).

The tumor responses depicted in Figure 11 B shows a significant improvement in long-term cure in combination with PDT and cisplatin. For combination therapy, 1h after PDT treatment, the mice injected with cisplatin 2.5 -5 mg/kg intra peritoneally (IP) weekly x 3 weeks and tumor regrowth were measured three times a week following the IACUC-approved animal protocol. Once the mice reach a tumor size >400 mm$^3$, they are euthanized. The results illustrated in Figure 11 (A & B) show a significantly improved long-term tumor cure of mice in combination of PDT with Cisplatin treatment

© 2026 by the author(s). Distributed under a Creative Commons CC BY license.

Preprints.org (www.preprints.org) | NOT PEER-REVIEWED | Posted: 19 June 2026 doi:10.20944/preprints202606.1473.v1



over the PDT alone in treating lung cancer (NSCLC). The therapeutic potential of **PS 531** was also evaluated in another lung Adenocar cinoma 15021, the PS dose was kept constant, and cisplatin dose was varied (e.g., 2.5 mg/kg x1, 2.5 mg/kg/weekly IP x 3 weeks IP and compared with cisplatin alone (2.5 mg/kg x 1IP) and 2.5 mg/kg x 3 weeks IP. As can be seen from the data summarized in Figure 11B, cisplatin for a chemotherapy treatment alone was less effective at a dose of 2.5 mg/kg. However, at the same dose, in combination with PDT improved tumor cure were obtained, Interestingly, 100% cure was observed at a PS dose of 1.0 mmol/kg, light dose: 135J/Cm$^2$, 75 mW/Cm$^2$ and the cisplatin dose of 2.5 mg/kg weekly x 3 weeks.

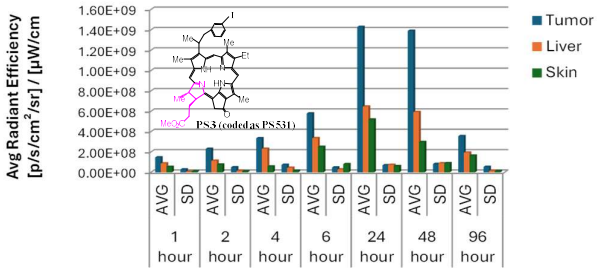


**Figure 11.** In vivo biodistribution of iodinated PS (dose: 1.0 mmol/kg) at various time points in SCID mice (3 mice/group) bearing NSCLC 148070 lung xenografts Ex:640/Em680 nm.

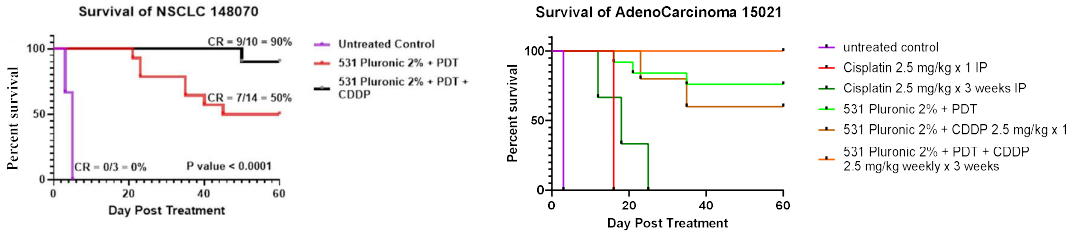


**Figure 12.** In vivo PDT efficacy of the iodinated PS (531) in SCID mice bearing lung tumor derived from patients' tumors (NSCLC 148070 and Adenocarcinoma 15021) with and without Cisplatin at variable doses and time intervals. PS and light doses and time of light exposure (PS dose:1.0 mmol/kg, light dose: 665 nm, 135 J/Cm$^2$, 75 mW/Cm$^2$ at 24 h post-injection of the PS (intravenously). For details, please see the text. P values were <0.0001 and the survival curves show significant difference. CDDP: cis-diammminedichloroplatinum (II) or cisplatin.

## 4. Conclusions

The work presented in this article demonstrates that the PDT efficacy of effective PSs, e.g., **HPPH**, and the iodinated **PS 531**, which are currently at various phases of clinical development, can further be enhanced by combination with cisplatin-chemotherapy. However, conjugation of HPPH either with *cis*- or *trans-platin* showed less uptake in cancer cell line and reduced cell destruction. Cisplatin even at less than therapeutic dose(s) in combination with HPPH-PDT or 531-PDT showed 80 to 100% tumor cured in mice bearing patients derived tumors. This study suggests that HPPH-PDT followed by cisplatin-chemotherapy increases tumor response (cure) significantly. The amount of chemotherapy drug needed for tumor destruction at the PDT dose of the PS-cisplatin conjugate was not enough for tumor destruction. It is also not advisable to increase the dose of the conjugate significantly, as it could lead to systemic toxicity, especially skin phototoxicity. Thus, the current findings suggest that for designing effective candidates for PDT, by covalently conjugating the PS with chemotherapy agent(s) may have limited clinical potential. Therefore, it could be useful in designing PDT clinical protocols in combination with FDA approved chemotherapy agent(s) for treating tumors with a significant synergetic impact.

© 2026 by the author(s). Distributed under a Creative Commons CC BY license.

Preprints.org (www.preprints.org) | NOT PEER-REVIEWED | Posted: 19 June 2026 doi:10.20944/preprints202606.1473.v1



**Supplementary Materials:** The following supporting information can be downloaded at the website of this paper posted on Preprints.org.

**Author Contributions:** Mykhaylo Dukh PhD, synthesized the photosensitizers, Farukh Durrani MBBS, evaluated the compounds with and without cisplatin chemotherapy in vivo, Joseph Cacaccio MS, performed the in vitro efficacy of the compounds, Walter A. Tabaczynski MS, Characterized the compound by NMR and mass spectrometry analyses, Mehrgan Ghazaeian (PhD student) helped in certain in vitro experiments, Heinz Bauman PhD conducted experiments and analyze the tumor-specificity data using 2D/3D cell culture systems, Ravindra Pandey PhD, provided the concept of the proposal, writing the original draft, generating resources and funds (Pandey & Baumann) for conducting the experiments and provided overall supervision. All authors including Paras Prasad PhD, helped in editing the manuscript.

**Institutional Review Board Statement:** All experiments related to in-vivo studies presented in this article were conducted by following the protocols approved by the IACUC committee of Roswell Park Comprehensive Cancer Center Institute, Buffalo, NY. (Ethics Approval Numbers: 537 M).

**Data Availability Statement:** The original contributions presented in this study are included in the article/supplementary material. Further inquiries can be directed to the corresponding author(s).

**Acknowledgments:** The authors are highly thankful for the financial support provided by the NIH PO1CA55791 (Pandey & Baumann), Photolitec, LLC (Pandey). Partial support of the shared resources of the Roswell Park Comprehensive Cancer Center support grant is also appreciated.

**Conflicts of Interest:** The authors declare no conflict of interest.

## References

1. Dasari S, Tchounwou B. P. Cisplatin in cancer therapy; molecular mechanisms of action. *Eur. J. Pharmacol.,* **2014,** *740*, 364-378.
2. Elmorsey E. A., Saber S, Hamad B. S., Abdel-Rehnin M. A., El-kott A. F., Alshehri M. A., Morsy K, Salama S. A., Yousef M. E. *European Journal of Pharmaceutical Sciences,* **2024**, *203*, 106939.
3. Coffetti G., Moraschi M., Facchetti G., Rimoldi I. The challenging treatment of cisplatin-resistant tumors: State of the art and future perspective. *Molecules,* **2023,** *28(8),* 3407
4. Yimit A., Adebali O, Sancar A., Jiang Y. Differential damage and repair of DNA-adducts induced by anti-cancer drug cisplatin across mouse organs. *Nature Communications,* **2019**, *10*, 309.
5. Chattaraj A., Syed M. P., Low C. A. Owonikoko T. K. Cisplatin-induced ototoxicity: A concise review of the burden, prevention and interception strategies. *JCO Oncology Practice,* **2023**, *19,* 278-283.
6. Bahremand K., Aghaz F., Bahrami K. Enhancing cisplatin efficacy with low toxicity in solid bladder cancer cells using pH-charge reversal sericin based nanocarriers: Development, characterization, and in vivo biological assessment. *ACS Omega,* **2024,** *9(12).* 14017-14032.
7. Li K., Li J., Li Z., Men L., Zuo H., Gong X. Cisplatin-based combination therapies: Their efficacy with a focus on ginsenosides co-administration. *Pharmacological Research*, **2024**, 107175.
8. Araghi M, Mannani R, Maleki A. H., Hamidi A., Rostami S., Safa S. H., Faramazi F., Khorasani S., Alimohammadi M., Tahmasebi S., Sigari R. A. Recent advances in non-small cell lung cancer targeted therapy; an update review. *Cancer Cell International*, **2023**, *23*, 162.
9. Thandra K. C., Barsouk A., Saginala K., Aluru J. S., Barsouk A. Epidemiology of lung cancer *Contemp. Oncol. (Pazn),* **2021**, *25(1),* 45-52.
10. Wu X., Zhang J., Yoshida Y. Disentangling the effects of various risk factors and trends in lung cancer mortality. *Scientific Reports,* **2025,** *15,* 8719.
11. Balbi, Cottin V., Singh S. Smoking-related lung diseases: a clinical perspective. *European Respiratory Journal,* **2010**, *35(2),* 231-233
12. Bosil M. C., Alysandratos K-D, Kotton D. N. Morrisey E. E. Lung repair and regeneration: Advanced models and insights into human disease. *Cell Stem Cell.* **2024**, *31*, 439-454.
13. Crous A., Abrahamse H. Photodynamic therapy of lung cancer, where are we? *Front Pharmacol.* **2022**, *13,* 932098.

© 2026 by the author(s). Distributed under a Creative Commons CC BY license.

Preprints.org (www.preprints.org) | NOT PEER-REVIEWED | Posted: 19 June 2026 doi:10.20944/preprints202606.1473.v1




14. Kan D., Ding R., Yang H., Jia Y., Lei K., Wang Z., Zhang W., Yang C., Liu Z and Xie F. Synergetic strategies in photodynamic combination therapy for cancer: mechanism, nanotechnology, and clinical translation. *Front. Oncol.* **2025**, *15*, 1607259.
15. Alvarez N, Sevilla A. Current advances in photodynamic therapy (PDT) and the future. Potential of PDT-combinational cancer therapies. *Int. J. Mol. Sci*., **2024,** 25(2), 1023.
16. Loewen G. M., Pandey R., Bellnier D., Henderson B. W., Dougherty T. Endobronchial photodynamic therapy for lung cancer. *Lasers Surg Med.* **2006,** *38(5),* 364.
17. Wang K., Yu B., Pathak J. An update in clinical utilization of photodynamic therapy for lung cancer. *J. Cancer*., **2021**, *12(4),* 1154-1160.
18. Pandey R. K. Zheng G. Porphyrins as photosensitizers in photodynamic therapy. The Porphyrin Handbook (Eds. Kadish K.M., Smith K. M., Guilard R.). *The porphyrin Handbook,* Academic Press, San Diego, CA, USA, **2000**, *6*, 157-230.
19. Ning S., Yaa Y., Feng X., Tian Y. Recent advances in developing bio-orthogonally activatable photosensitizers for photodynamic therapy. *European Journal of Medicinal Chemistry*, **2025,** *291*, 117672.
20. Muskovic M., Loncarie M, Ratkaj I, Malatesti N. Impact of the hydrophilic-lipophilic balance of free-based and Zn(II) tri-cationic pyridinium porphyrins and irradiation wavelength in PDT against the melanoma cell lines. *European Journal of Medicinal Chemistry*, **2025**, *282*, 117063.
21. Ethirajan M., Chen Y., Joshi P and Pandey, R. K. The role of porphyrin chemistry in tumor imaging and photodynamic therapy. *Chem. Soc. Rev.*, **2011,** *40,* 340-362.
22. Pandey R. K., Goswami L. N., Chen Y., Gryshuk A., Missert J. R., Oseroff A., Dougherty, T. J. Nature: a rich source for developing multifunctional agents. Tumor-imaging and photodynamic therapy. *Lasers Surg Med.* **2006**, *38(5),* 445-467.
23. Rigual N., Shafirstein G, Cooper M. T., Baumann H., Bellnier D. A., Sunar U., Tracy E. C., Rohrbach D. J., Wilding G., Yan W., Sullivan M., Merzianu M., Henderson B. W., Photodynamic therapy with 3-(1'-hexyloxyethyl) pyropheophorbide-a for cancer of the oral cavity. *Clinical Cancer Research,* **2013**, *19(23),* 6605-6613.
24. Nava H. R., Alemanni S. S., Dougherty T. J., Cooper M. T., Ian W., Wilding G., Henderson B. W. Photodynamic therapy (PDT) using HPPH for the treatment of precancerous lesions associated with Barrett's esophagus. *Lasers Surg Med.* **2011**, *43(7),* 705-712.
25. Patel N., Pera P., Joshi P., Dukh M., Siters K. E., Kryman M., Charuku R. R., Durrani F. A., Missert J. R., Warson R., Ohulchanskyy T. Y., Tracy E. C., Baumann H and Pandey R. K. Highly effective dual-function near-infrared (NIR) photosensitizer for fluorescence imaging and photodynamic therapy (PDT) of cancer. *J. Med. Chem.*, **2016**, *59 (21)*, 9774-9787.
26. Pandey S. K., Gryshuk A. L., Sajjad M., Zheng X., Chen Y., Abouzeid M. M., Morgan J., Charamisinau I., Nabi H. A., Oseroff A., Pandey R. K. Multimodality agents for tumor imaging (PET, fluorescence) and photodynamic therapy: A possible "see and treat" approach. *J. Med. Chem.,* **2005**, *48(20),* 6286-6295.
27. Gupta A., Wang S., Marko A., Joshi P., Ethirajan M., Chen Y., Yao R., Sajjad M., Kopelman R., Pandey R. K. Polyacrylamide-based biocompatible nanoplatform enhances the tumor uptake, PET/fluorescence imaging and anticancer activity of a chlorophyll analog. *Theranostics,* **2014**, *4(6),* 614-628.
28. Srivatsan A., Para P., Joshi P, Marko A. J., Durrani F., Missert J. R., Curtin L., Sexton, S., Yao R., Sajjad M and Pandey R. K. Highlights on the imaging (nuclear fluorescence) and phototherapeutic potential of a tri-functional chlorophyll-a analog with no significant toxicity in mice and rats. *Journal of Photochemistry and Photobiology B: Biology*, **2020**, *11*, 111998.
29. Durrani F. A., Cacaccio J., Turowski S. G., Dukh M., Bshara W., Curtin L., Sexton S., Spernyak J., Pandey R. K. Photobac derived from bacteriochlorophyll-a shows potential for treating brain tumor in animal models by photodynamic therapy with desired pharmacokinetics and limited toxicity in rats and dogs. *Biomedicine & Pharmacology*, **2023**, *168*, 115731.
30. Dhiman V. K., Kumari M., Singh D. Chemoresistance: The hidden barrier in cancer treatment. *Cancer Pathogenesis and Therapy*, **2026**, *4(2),* 98-108.
31. Chhabra N., Aseri M. L., Padmanabhan D. A review of drug isomerism and its significance. *Int. J. Appl. Basic Med Res*. **2013**, *3(1),* 16-18.


© 2026 by the author(s). Distributed under a Creative Commons CC BY license.

Preprints.org (www.preprints.org) | NOT PEER-REVIEWED | Posted: 19 June 2026 doi:10.20944/preprints202606.1473.v1




32. Kishimoto T., Yoshikawa Y., Yoshikawa K., Komeda S. Different effects of cisplatin and transplatin on the higher order structure of DNA and gene expression. *Int. J. Mol. Sci.,* **2019**, *21(1),* 34.
33. Saenz C., Cheruku R. R., Ohulchanskyy T. Y., Joshi P., Tabaczynski W. A., Missert J. R., Chen Y., Pera P., Tracy E., Marko A., Rohrbach D., Sunar U., Baumann H., Pandey, R. K. Structural and Epimeric isomers of HPPH: Effects on uptake and photodynamic therapy of cancer. *ACS Chem. Biol.* **2017,** *12(4),* 933-946.
34. Bellnier D. A., Greco W. R., Loewen G. M., Nava H., Oseroff A. R., Pandey R. K., Tsuchida T, Dougherty T. J. Population pharmacokinetics of the photodynamic therapy agent 2-(1-hexyloxyethyl)-2-devinylpyropheophorbide-a in cancer patients. *Cancer Res.* **2003,** *63(8),* 1806-1813.
35. Cheruku R. R., Cacaccio J., Durrani F. A., Tabaczynski W. A., Watson R., Siters K., Missert J. R., Tracy E. C., Guru K, Koya R. C., Kalinski P., Baumann H., Pandey, R. K. Synthesis, Tumor-Specificity and Photosensitizing Efficacy of Erlotinib Conjugated Chlorins and Bacteriochlorins: Identification of a Highly Effective Candidate for Photodynamic Therapy of Cancer. *J. Med. Chem.* **2021**, *64*, 741−767.
36. Kessel D., Luo Y., Mathieu P., Reiners J. J. Determinants of the apoptotic response to lysosomal photodamage. *Photochem. Photobiol.* **2000**, *71(2),* 196-200.
37. Henderson B. W., Bellnier D. A., Greco W. R., Sharma A., Pandey R. K., Vaughan L., Weishaupt K. R. and Dougherty T. J. An in vivo QSAR for a congeneric series of pyropheophorbide derivatives as photosensitizers for photodynamic therapy. *Cancer Res.* **1997**, *57(18),* 4000-4007.
38. Messori L., Merlino A. Cisplatin binding to proteins: A structural perspective. *Coordination Chemistry Reviews*. **2016,** *315*, 67-89.
39. Tracy E. C., Bowman, M-J., Pandey R. K. and Baumann H. Tumor cell-specific retention of photosensitizers determines the outcome of photodynamic therapy for head and neck cancer. H. *Photochem. Photobiol. B: Biology*, **2022**, *234*, 112513.
40. Zhang S., Patel N. J. and Pandey R. K. Chlorophyll-a analogs for cancer-imaging and therapy (Theranostics). *Top. Heterocyclic Chemistry*, **2014,** *34,* 1-30, Edited by Professor Roberto Paolesse (Editor) Applications of Porphyrinoides, Springer, New York.


**Disclaimer/Publisher's Note:** The statements, opinions and data contained in all publications are solely those of the individual author(s) and contributor(s) and not of MDPI and/or the editor(s). MDPI and/or the editor(s) disclaim responsibility for any injury to people or property resulting from any ideas, methods, instructions or products referred to in the content.

© 2026 by the author(s). Distributed under a Creative Commons CC BY license.